

Comparative analysis of *Neph* gene expression in mouse and chicken development

Linus A. Völker · Marianne Petry · Mohammad Abdelsabour-Khalaf · Heiko Schweizer · Faisal Yusuf · Tilman Busch · Bernhard Schermer · Thomas Benzing · Beate Brand-Saberi · Oliver Kretz · Martin Höhne · Andreas Kispert

Accepted: 10 December 2011 / Published online: 29 December 2011
© The Author(s) 2011. This article is published with open access at Springerlink.com

Abstract Neph proteins are evolutionarily conserved members of the immunoglobulin superfamily of adhesion proteins and regulate morphogenesis and patterning of different tissues. They share a common protein structure consisting of extracellular immunoglobulin-like domains, a transmembrane region, and a carboxyl terminal cytoplasmic tail required for signaling. Neph orthologs have been widely characterized in invertebrates where they mediate such diverse processes as neural development, synaptogenesis, or myoblast fusion. Vertebrate Neph proteins have been described first at the glomerular filtration barrier of the kidney. Recently, there has been accumulating evidence suggesting a function of Neph proteins also outside the kidney. Here we demonstrate that *Neph1*, *Neph2*, and *Neph3* are expressed differentially in various tissues during ontogenesis in mouse and chicken. *Neph1*

and *Neph2* were found to be amply expressed in the central nervous system while *Neph3* expression remained localized to the cerebellum anlage and the spinal cord. Outside the nervous system, *Neph* mRNAs were also differentially expressed in branchial arches, somites, heart, lung bud, and apical ectodermal ridge. Our findings support the concept that vertebrate Neph proteins, similarly to their *Drosophila* and *C. elegans* orthologs, provide guidance cues for cell recognition and tissue patterning in various organs which may open interesting perspectives for future research on Neph1-3 controlled morphogenesis.

Keywords Neph1 · Neph2 · Neph3 · SYG-1 · SYG-2 · Kirre-like · IrreC/Rst

L. A. Völker · B. Schermer · T. Benzing · M. Höhne
Department II of Internal Medicine and Center for Molecular
Medicine, University of Cologne, 50937 Cologne, Germany

M. Petry · A. Kispert
Institute for Molecular Biology, Medizinische Hochschule
Hannover, 30625 Hannover, Germany

M. Abdelsabour-Khalaf · F. Yusuf · B. Brand-Saberi
Department of Anatomy and Molecular Embryology,
Medical Faculty, Ruhr University,
44801 Bochum, Germany

H. Schweizer · T. Busch
Renal Division, University Hospital Freiburg,
79106 Freiburg, Germany

B. Schermer · T. Benzing
Cologne Excellence Cluster on Cellular Stress Responses
in Aging-Associated Diseases, University of Cologne,
50937 Cologne, Germany

O. Kretz
Department of Neuroanatomy, Institute of Anatomy
and Cell Biology, University of Freiburg,
79104 Freiburg, Germany

M. Höhne (✉)
Nephrologisches Forschungslabor, Uniklinik Köln, Kerpener Str.
62, Gebäude 15, 1. Obergeschoss, 50937 Cologne, Germany
e-mail: martin.hoehne@uk-koeln.de

A. Kispert (✉)
Institut für Molekularbiologie, OE5250, Medizinische Hochschule
Hannover, Carl-Neuberg-Str. 1, 30625 Hannover, Germany
e-mail: kispert.andreas@mh-hannover.de

Introduction

Neph proteins are members of the immunoglobulin superfamily (IgSF), a class of cell–cell-recognition molecules that share a variable number of extracellular immunoglobulin-like domains as a common structure and interact with other IgSF-proteins in a homophilic or heterophilic way. In addition to Neph proteins, the IgSF also comprises neural cell adhesion molecules (NCAMs), integrins, receptor tyrosine kinases, plexins, neuroligins, neuexins, and neuropilins, molecules with a proven role in cell recognition and tissue patterning. These proteins have been shown to be involved in a wealth of ontogenetic mechanisms including synapse formation and axonal pathfinding, cell migration, myoblast fusion, epithelial cell sorting, and cell fate determination [reviewed in (Maness and Schachner 2007)]. All Neph proteins consist of five extracellular Ig-like domains, a transmembrane domain, and a cytoplasmic tail that contains a podocin-binding motif, a PDZ binding motif, and a SH2-binding site (Sellin et al. 2003). Together with the closely related IgSF protein Nephrin, Neph proteins play a pivotal role for the development and maintenance of the filtration barrier in the kidney (Donoviel et al. 2001; Kestila et al. 1998; Neumann-Haefelin et al. 2010). Neph1 has been shown to interact with Nephrin at the glomerular slit diaphragm, a specialized cell junction of kidney podocytes, the visceral epithelial cells of the kidney (Barletta et al. 2003; Liu et al. 2003). With primary and hundreds of interdigitating secondary processes podocytes enwrap the glomerular capillaries. The extracellular domains of Nephrin and Neph1–3 bind to each other in a heterophilic and homophilic manner constituting a protein complex localized at the slit diaphragm (Gerke et al. 2005; Ihalmo et al. 2003). Mutations in the *Nephrin* gene cause a congenital nephrotic syndrome in humans (Kestila et al. 1998) and deletion of *Neph1* was found to cause severe glomerular disease and perinatal death in mice (Donoviel et al. 2001). In contrast to Neph1, the role of Neph2 and Neph3 in podocyte biology is much less clear. Neph2 and Neph3 were detected at the glomerular slit diaphragm by immunogold and immunofluorescent staining (Gerke et al. 2003; Ihalmo et al. 2003). Basal expression of *Neph3* in podocytes is driven by NFkappaB and SP-1, while the transcription factors upstream of *Neph1* and *Neph2* in the podocyte have remained unclear (Ristola et al. 2009). Soluble fragments of Neph2 were found in urine of healthy individuals due to cleavage of its extracellular domain by metalloproteinases under physiological conditions (Gerke et al. 2005). All mammalian Neph proteins bind the slit diaphragm protein podocin and have been implicated in slit diaphragm centered signaling (Sellin et al. 2003).

Additional functions of Neph proteins have been identified and extensively studied in the model organisms

D. melanogaster and *C. elegans*. Initial studies in *D. melanogaster* demonstrated a role for the Neph1 ortholog IrreC/Rst in axonal guidance in the optic chiasm (Ramos et al. 1993; Schneider 1995). These studies revealed restricted homophilic interactions of IrreC/Rst to be required for the correct projection of optical lobe neurons, while overexpression or knock-out leads to erroneous axonal pathfinding. In addition, the two orthologs of Neph1, Kirre and IrreC/Rst (*rst*) and the two orthologs of Nephrin, Sticks-and-Stones (SNS) and Hibris (Hbs), have been shown to mediate cell–cell recognition in muscle development. In *Drosophila* embryos, they interact in a *trans*-heterophilic binding to establish contacts between myoblast founder cells expressing the Neph1 orthologs Kirre/Rst and fusion-competent myoblasts (FCM) expressing the Nephrin orthologs SNS/Hbs. This interaction initiates myoblast fusion to form the final *Drosophila* muscle units (Chen and Olson 2004; Menon et al. 2005; Ruiz-Gómez et al. 2000; Strunkelberg et al. 2001). Another process regulated by Neph protein orthologs in the fly that has been investigated very systematically in the past decade is the development of the eye. In the pupal eye disc, *rst* and *hbs* are necessary to pattern epithelial cells into the precise ommatidial array. This involves the preferential adhesion between interommatidial precursor cells and primary pigment cells that express Rst or Hbs, respectively (Bao and Cagan 2005). Cell–cell recognition is also the main function of the *C. elegans* orthologs of Nephrin and Neph1 (SYG-2 and SYG-1). SYG-1 and SYG-2 have been shown to determine the target-specific synaptogenesis of the HSN neuron (hermaphrodite specific motor neuron) onto vulval epithelial cells (Shen et al. 2004). Site-specific cell recognition through the interaction of SYG-2 on guidepost cells and SYG-1 on HSN-type neurons protects on-target synaptic proteins from E3 ubiquitin ligase-mediated degradation and thus restricts synapses to a demarcated region on the HSN neuron. In conclusion, the Neph orthologs in *D. melanogaster* and *C. elegans* constitute signaling modules that mediate cell–cell recognition and cell sorting in tissue morphogenesis, axonal pathfinding, and synaptic plasticity (Fischbach et al. 2009; Huber and Benzing 2005).

Recent studies on Neph protein function in extrarenal organ systems revealed that mammalian Neph proteins have similar cell–cell recognition functions. Nephrin and Neph3 expression is driven by the transcription factor Ptf1a in the cerebellum (Mizuhara et al. 2010). Neph3 expressing cells constitute two GABAergic neuronal precursor subpopulations in the rhombic lip, the site of cerebellogenesis, that later differentiate into Purkinje cells of the cerebellar cortex or into neurons of the deep cerebellar nuclei (Minaki et al. 2005; Nishida et al. 2010). A mechanism of how Neph proteins mediate cell–cell-recognition in neuronal tissue has been further clarified in the olfactory system. Here

Neph2 and Neph3 are expressed in an antidromic way in certain subsets of olfactory sensory neurons displaying different olfactory receptors. Neph2 and Neph3 bundle axons of similar olfactory sensory neurons by homophilic interaction and cause them to converge in a specific set of olfactory glomeruli (Serizawa et al. 2006). Similar mechanisms might be involved in organizing the topology of the optical chiasmata in *Drosophila* (Clandinin and Zipursky 2002; Schneider 1995; Sugie et al. 2010). Interestingly, patients with a defect in the transcription factor Ptf1a, which acts upstream of Neph3, exhibit cerebellar and pancreatic agenesis and neonatal diabetes mellitus, suggesting a possible role of Neph3 in pancreas and cerebellar development (Hoveyda et al. 1999; Sellick et al. 2004).

Taken together, Neph and Neph3 protein complexes serve as conserved signaling modules that regulate cell–cell recognition and tissue morphogenesis. This module has been shown to be of critical importance for the development and maintenance of several tissues. However, the respective target tissues in vertebrates are still ambiguous. To identify further tissues and organs that require Neph function for morphogenesis and patterning, we performed a comprehensive and systematic analysis of Neph mRNA expression in mice and chicken.

Materials and methods

Animals

Pregnant NMRI mice were killed at appropriate developmental stages [Embryonic day (E) 9.5, E10.5, E11.5, E12.5, E14.5, E16.5] to obtain embryos. Fertilized chicken eggs were staged according to Hamburger-Hamilton (HH) by somite number. All experiments were performed according to the guidelines of animal welfare at our institution.

Histology and tissue preparation

Isolated embryos were fixed in 4% paraformaldehyde solution overnight, dehydrated in phosphate-buffered saline (plus Tween-20; PBT) of increasing methanol concentrations for use as whole-mount embryos, and stored in 100% methanol at -20°C . For histological sections, phosphate-buffered saline (PBS) of increasing ethanol concentrations was used instead, and samples were embedded in paraffin. 8- μm sections were cut using a microtome (Leica).

In situ hybridization

A mouse kidney cDNA library and a chicken cDNA library served to clone fragments of coding sequence and 3'-untranslated region of mouse *Neph1*, *Neph2*, *Neph3*, and

chicken homologues of *Neph1* and *Neph2*. The following primers were used: Mouse: *Neph1/Neph2*: as described previously (Gerke et al. 2006). *Neph3*: forward primer 5'-CG CCATGGCTCTCTCTCTAAGC-3', reverse primer 5'-TC ACACATGAGTCTGGAGACGCTGGT-3' Chicken: *gga-Neph1*: forward primer 5'-ACCCACCGTCACCGACAT-3', reverse primer 5'-TGCTTCAAGTCCACGTCATC-3' on template ENSGALT00000010117; *gga-Neph2*: forward primer 5'-CATTGTGCTGTGGATCAAGG-3', reverse primer 5'-G TCAGAGCCAAAGCTGTTCC-3' on template ENSGALT 00000041073. PCR fragments were inserted into *pBluescript SK+* vector (Invitrogen, Carlsbad, CA) using NotI and MluI restriction sites. *pBluescript SK+* vector was linearized and digoxigenin-(DIG)-labeled antisense riboprobes were generated using T7-RNA-polymerase (Ambion).

For whole-mount in situ hybridization (ISH) analysis, embryos were progressively rehydrated, digested with proteinase K (1:1,000, 10–45 min according to sample size), and refixed in 4% PFA/0.2% glutaraldehyde for 20 min. After prehybridization (60 min), hybridization with DIG-UTP probes took place overnight in standard saline citrate (SSC; pH 4.5; containing 50% formamide) at 65–70°C. Specimens were then incubated with alkaline phosphatase-conjugated anti-DIG Fab fragments (Roche, Mannheim, Germany) at a dilution of 1:4,000 overnight at 4°C. Alkaline phosphatase was detected using chromogenic conversion of NBT/BCIP (Roche).

For vibratome sections, whole-mount embryos were stored in 4% PFA after in situ hybridization. Embryos were embedded in heated fluid 3–4% agarose. After cooling for 1 h at room temperature, sectioning was performed with a vibratome at 35–50 μm .

For paraffin section ISH, slides were progressively rehydrated and permeabilized with proteinase K for 3 min. Prehybridization, hybridization, and detection were carried out as described above. To avoid drying up of the slides during hybridization, we placed them in a humidity chamber containing 5 \times SSC and 40% formamide. Slides were then progressively dehydrated, washed in xylol, and mounted.

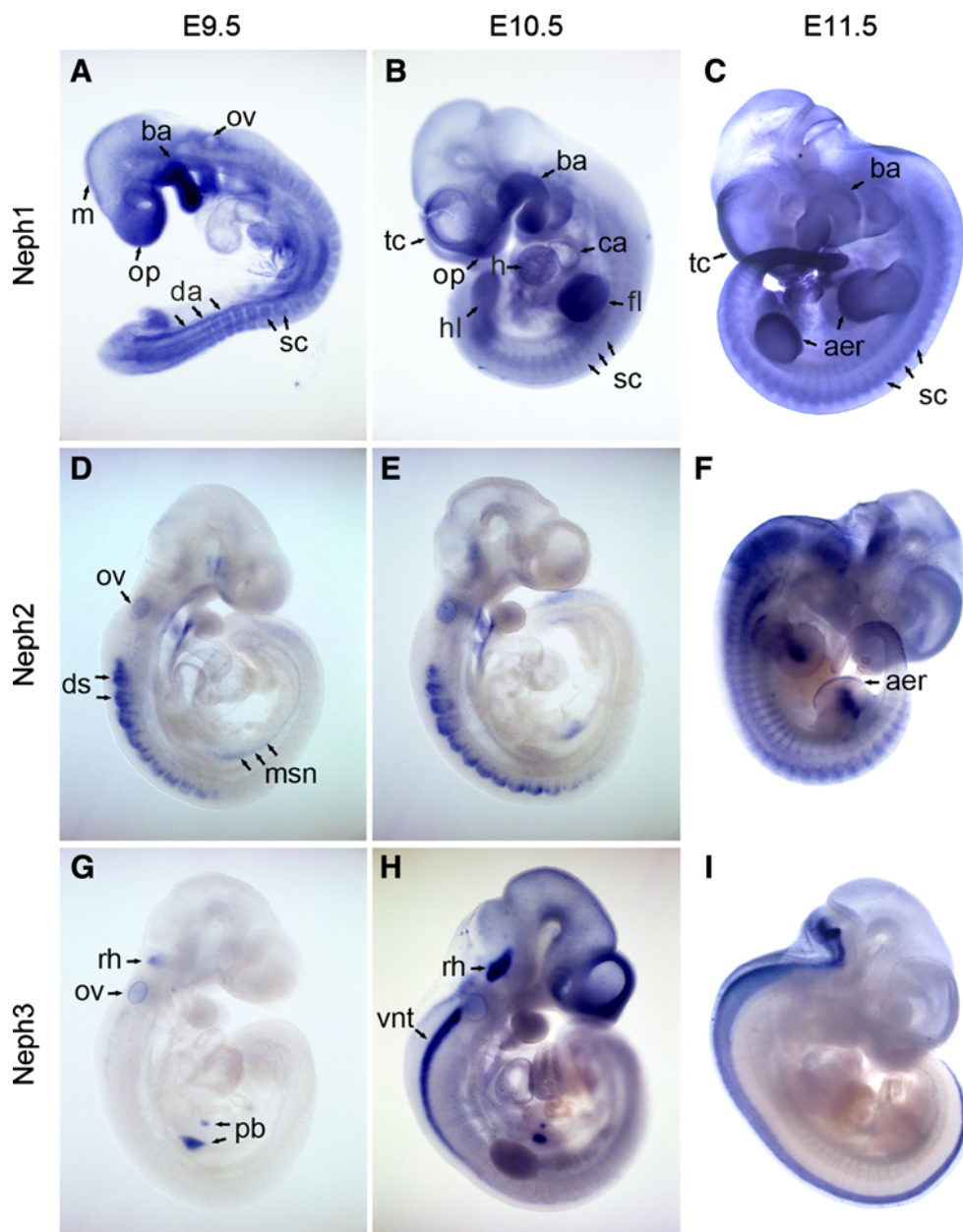
Digital images were taken on a stereomicroscope (Leica MZ8) equipped with a digital camera. For figure preparation, brightness and contrast were adjusted using Photo-shop.

Results

Expression analysis of *Neph1* during mouse development

To analyze *Neph* mRNA expression, we performed in situ hybridization studies using murine embryos of different developmental stages. Whole-mount in situ hybridization of E9.5–E11.5 embryos revealed persistent expression of

Fig. 1 Whole-mount in situ hybridization analysis of *Neph1* (a–c), *Neph2* (d–f), and *Neph3* (g–i) expression in mouse embryos at E9.5 (a, d, g), E10.5 (b, e, h), and E11.5 (c, f, i). Blue NBT/BCIP precipitates are indicative of mRNA expression. *aer* apical ectodermal ridge, *ba* branchial arch, *ca* common atrium, *da* dorsal aorta, *ds* dorsal somite, *fl* fore limb, *h* heart, *hl* hind limb, *m* mesencephalon, *msn* mesonephros, *vnt* ventral neural tube, *op* olfactory placode, *ov* otic vesicle, *pb* pancreatic bud, *rh* rhombencephalon, *sc* sclerotom, *tc* teloclele



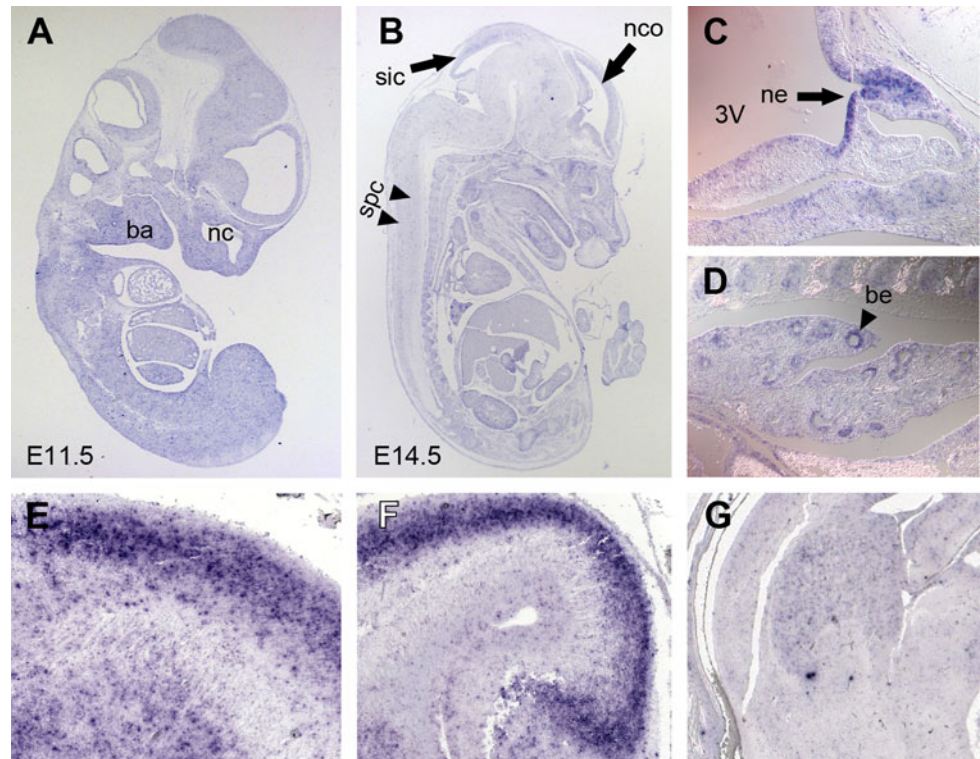
Neph1 transcripts in the olfactory placode, branchial arches, and somites (Fig. 1a–c). In the developing mouse brain, intense *Neph1* expression was visible in the teloclele.

Specifically at E9.5 (Fig. 1a), two long streaks of *Neph1*-positive cells aligned with the somites at their ventral edge. This expression pattern correlates best with the dorsal aortae, which extend to the tip of the tail, and are in the process of uniting to become the unpaired abdominal aorta at this stage of development. In addition, *Neph1* mRNA was detected around the otic vesicle. However, this did not persist at later stages. In the course of embryonic development, expression intensity increased in the left ventricle and the common atrium of the heart. The limb buds were also positive for *Neph1* from E9.5 to E11.5 without discriminating

particular zones (Fig. 1b). At E11.5, an increased level of *Neph1* was found at the apical ectodermal ridge at the extremity of the buds (Fig. 1c). Interestingly, the initially broad expression in the central nervous system became restricted at E11.5 to the now paired telocleles leaving mesencephalon and rhombencephalon almost void of expression.

Hybridization on paraffin sections of mouse embryos allowed for a more detailed analysis of *Neph1* expression domains. At stage E11.5, we detected almost ubiquitous expression with locally increased intensity in the areas of the nasal pit and the branchial arches (Fig. 2a). With proceeding embryonic development, *Neph1* expression in the neocortex and the superior and inferior colliculi of the

Fig. 2 In situ hybridization analysis of *Neph1* expression. Paramedian sagittal section of E11.5 (a) and E14.5 (b) mouse embryos. Ubiquitous expression of *Neph1* is detected in tissues derived from all three germ layers. Higher magnification of Rathke's pouch (c) and of the pseudoglandular lung anlage (d) at E12.5. *Neph1* expression is found in different regions of the developing brain at E16.5: neocortex (E sagittal); hippocampus (F sagittal); ganglionic eminence (G frontal). 3V third ventricle, ba branchial arches, nc nasal cavity, nco neocortex, ne neuroepithelium, spc spinal cord, sic superior and inferior colliculi of the mesencephalon



mesencephalon (Fig. 2b) became layer-specific, and two tracts of faintly *Neph1*-positive cells spanned the spinal cord in a cranio-caudal direction (Fig. 2b; E14.5). Also, small domains of the thalamus and the tegmentum stained positive. Higher magnifications of *Neph1*-positive cell bands in the developing neocortex (Fig. 2e), the hippocampus (Fig. 2f), and the ganglionic eminence (Fig. 2g) showed *Neph1* to be layer- or, as in case of the ganglionic eminence, population-specific since *Neph1*-negative cells seemed to be interspersed here. However, further investigation is needed to determine affiliation of *Neph1*-positive cells with particular layers or cell types, the more so as the brain at this point is remodeling rapidly, and neuronal cell populations migrate toward the marginal zone of the neocortex by passing through preexistent cell layers (Goffinet 1979).

Additional *Neph1* transcripts were detected at Rathke's pouch giving rise to the anterior pituitary lobe as well as at the base of the third ventricle in the neuroepithelium of the developing posterior lobe (Fig. 2c, ne—black arrow), and, intriguingly, in the epithelia of the developing bronchial system (Fig. 2d, black arrow head).

Expression pattern of *Neph2* in murine embryonic stages

Whole-mount in situ hybridization revealed an initially precisely circumscribed expression of *Neph2* transcripts, which became broader at later stages. At E9.5 (Fig. 1d) and E10.5 (Fig. 1e), the dorsal somites, the otic vesicle, and the

second and third branchial arches exhibited *Neph2* expression. Expression in the somatic mesoderm at these stages was limited to cranial somites and extended to the caudal somites in the course of embryonic development (Fig. 1f). The diencephalic neuroepithelium or the ectodermal epithelium of Rathke's pouch stained positive for *Neph2*, arguably suggesting a role for *Neph2* (in concert with *Neph1*) in the development of the pituitary gland. However, at this magnification expression cannot be easily ascribed to either anterior or posterior lobe. The mesonephros, a linear structure expressing *Neph2*, is visible ventral of the caudal somites at E9.5 (Fig. 1d), while at stage E10.5 the identity of this domain is unclear (Fig. 1e). With the transition to stage E11.5, major parts of the prosencephalon and the brain stem including pons, medulla oblongata, and the cranial segments of the spinal cord transition zone now stained positive for *Neph2* (Fig. 1f). Labeled cells were also found at the site of the primitive intervertebral discs. The anatomically most defined *Neph2* expression was localized to the apical ectodermal ridge of fore and hind limb buds and the limb mesenchyme as can be seen in more detail in Fig. 3a. Expression at the apical ectodermal ridge was also present at earlier stages while expression in the mesenchymal domain started later (Fig. 3b; E10.5 insert). Note that the kidney anlage is presumably covered by the hind limb.

We next sectioned mouse brains at stage E16.5. The overview (Fig. 3c) revealed a distinct expression pattern within the neocortex (Fig. 3d), the diencephalon (Fig. 3e, f), and the rhombencephalon (Fig. 3g). *Neph2* transcripts in

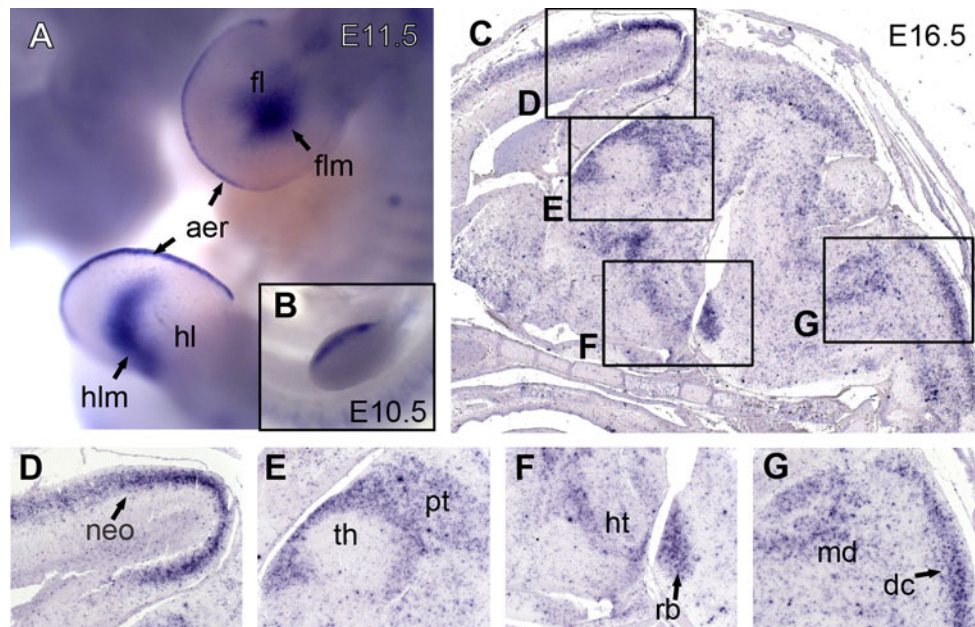


Fig. 3 *Neph2* expression as revealed by in situ hybridization analysis. Magnification of fore- and hindlimb buds of an E11.5 mouse embryo (a). Embryo is shown from the left, the back directed to the right. The insert shows earlier stage (E10.5) of fore limb development (b). Sagittal sections of mouse brain at stage E16.5 (c). Higher magnification of

neocortex (d), diencephalon (e), pons (f), and oblong medulla (g) as indicated by boxes. *aer* apical ectodermal ridge, *dc* dorsal column tract, *fl* fore limb; *flm* fore limb mesenchyme, *hl* hind limb, *hlm* hind limb mesenchyme, *ht* hypothalamus, *md* medulla, *neo* neocortex, *pt* pretectum, *rb* rhombomere basal plate

the neocortex (Fig. 3d) were localized in superficial layers. In the diencephalon at a paramedian section, *Neph2* mRNA was detected in the prethalamic region, the adjacent intermediate tier of the thalamus, and a small band of cells bordering the rostral part of the dorsal tier of the thalamus (Fig. 3e). Basal plates of rhombomeres at the rostral part of the ponto-medullary transition zone showed intense expression (Fig. 3f rb). Juxtaposed to this area, we also found staining in the peduncular hypothalamus (Fig. 3f ht).

At the spino-medullary transition, an oblong area of *Neph2* expression extended caudally into the spinal cord (Fig. 3g). This correlates best with the trigeminal column or the dorsal column tract. Marginally rostral of the cranial end of the column-shaped domain, a cell cluster with strong *Neph2* expression stood out. This may represent the alar plates of caudal rhombomeres.

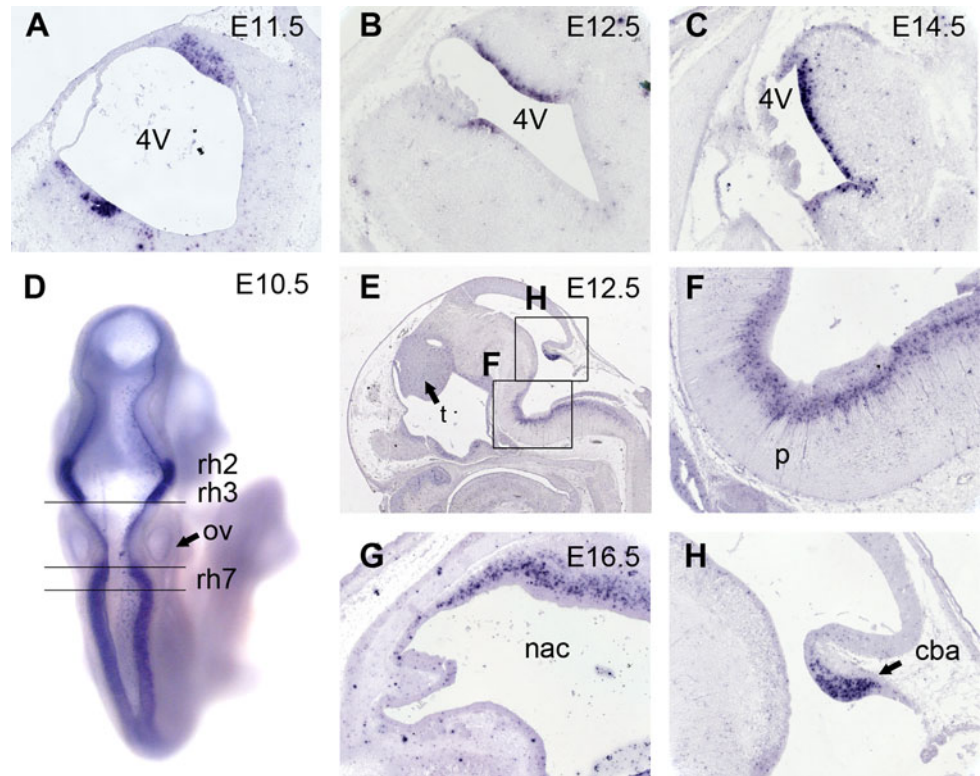
Expression of *Neph3* during mouse development

In comparison with the previously described expression domains of *Neph1* and *Neph2*, *Neph3* showed a more limited and highly specific expression in the whole-mount in situ hybridizations. While at stage E9.5 (Fig. 1g), *Neph3* was exclusively transcribed in cells of the otic vesicle, the pancreas bud, the metanephros, and a small area at the bottom of the fourth ventricle, expression at stage E10.5 (Fig. 1h) also included parts of the rhombencephalon,

differentiating cells of the neural crest and the telencephalon. Interestingly, expression in all structures except for the neuronal crest and the cerebellum anlage vanished completely at stage E11.5 (Fig. 1i) suggesting a rather specific role for *Neph3* in development.

Detailed analysis of *Neph3* expression domains in the CNS on paraffin sections identified a group of cells in the cranial roof and the floor of the fourth ventricle to be expressing *Neph3* at high levels (Fig. 4a). This expression was consistent throughout all of the screened stages (i.e. E11.5, E12.5, E14.5, Fig. 4a–c) and only widened slightly in the rostro-occipital axis. A dorsal view of a whole-mount specimen revealed the rhombomere-specific pattern in the neural crest (Fig. 4d; E10.5). Note the position of the otic vesicle next to rhombomere 5 as a point of orientation (Young et al. 2009). Rhombomeres r2, r3, and r7 stained for *Neph3* as did a thin layer of cells delineating the border of the single ependymal cell layer comprising the roof plate and the alar plate. A sagittal section of an E12.5 embryo (Fig. 4e) revealed *Neph3* expression domains in the entire thalamus, the cerebellum anlage, and the pontal flexure. On detailed analysis, *Neph3* positive cells at the pontal flexure extend processes towards the floor plates of the pertaining rhombomeres, while their cell bodies appeared to be ventricularly localized (Fig. 4f). This domain did not span the entire rhombencephalon but initiated cranially at the level of r2 in the pontine hindbrain and reached far into the

Fig. 4 In situ hybridization analysis of *Neph3* expression. Continued expression at the *bottom* and the roof of the fourth ventricle in E11.5 (a), E12.5 (b), and E14.5 (c) mouse embryos. Dorsal view of an E10.5 embryo (d) reveals rhombomere-specific expression. Note the position of the otic vesicle (ov). Sagittal section of an E12.5 embryo (e, f, h) with demarcated expression in the thalamus (t), the cerebellum anlage (cba), and cell populations in the pons (p). At a later time point (i.e. E16.5, g), cells populating the roof of the nasal cavity express *Neph3*. 4V fourth ventricle, cba cerebellum anlage, nac nasal cavity, ov otic vesicle, p pons, rh rhombomere, t thalamus



medullary hindbrain. In case of the expression domain in the cerebellum anlage, areas with highly elevated expression levels were distinguished from areas with almost no *Neph3* transcripts present. At higher magnification, these areas could be correlated with the external (*Neph3*-negative) and the internal germ layer (*Neph3*-positive) (Fig. 4h). Additionally, *Neph3* was also expressed at the roof of the nasal cavity, from where the olfactory epithelium extends axons towards the prosencephalon at this point of embryonic development and induces the olfactory bulb in the rostral part of the prosencephalon (Fig. 4g).

Expression of *Neph* homologues in chicken development

To check for an evolutionary preserved role of *Neph* proteins, we searched genome databases of *Gallus gallus* for homologues of *Neph* like genes. While *Neph1*, *Neph2*, and slit-diaphragm-associated *Podocin* were present, no homologues for *Nephrin* or *Neph3* could be detected (Fig. 5). Next, we conducted in situ hybridization analysis on chicken embryos at stages 20 and 23 according to Hamburger and Hamilton (HH). Strikingly, expression patterns did not vary greatly from those observed in mice. Expression of *Neph1* and *Neph2* homologues (consequently named *gga-Neph1* and *gga-Neph2*) included the central nervous system, kidney precursors, limb buds, otic vesicle, branchial arches, and, in case of *Neph2*, the heart and its outflow tract (Fig. 6).

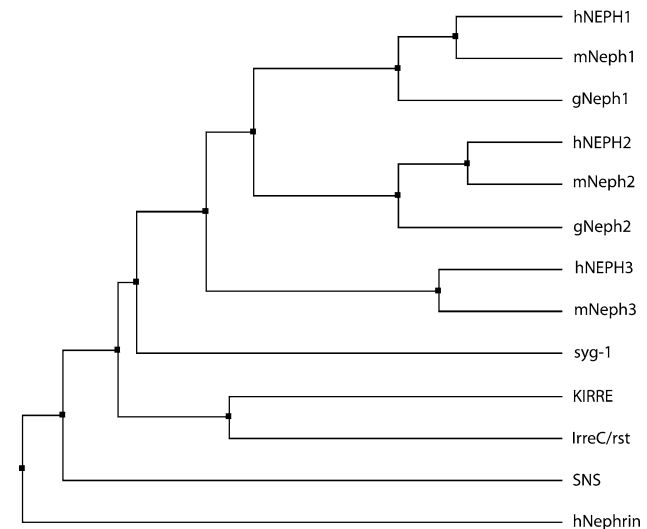


Fig. 5 Phylogenetic tree showing homology between Nephrin- and Neph-like genes in vertebrates and invertebrates as discussed in the text. Accession numbers used for analysis: *hNEPH1* AAI09194, *mNeph1* AAH23765, *gNeph1* ENSGALT00000010117, *hNEPH2* AAI01776, *mNeph2* AAH63072, *gNeph2* ENSGALT00000041073, *hNEPH3* AAP72166, *mNeph3* AAI58022, *syg-1* AAC47074, *KIRRE* AAF86308, *IrreC/rst* AAA16632, *SNS* AAF77184, *hNephrin* AAG17141

Gga-Neph1 was strongly expressed not only in the central nervous system, particularly in the telenceles and the mesencephalon, but also in the optic cup, the dorsal parts of the somites, and the limb buds. Expression of *gga-Neph1* in

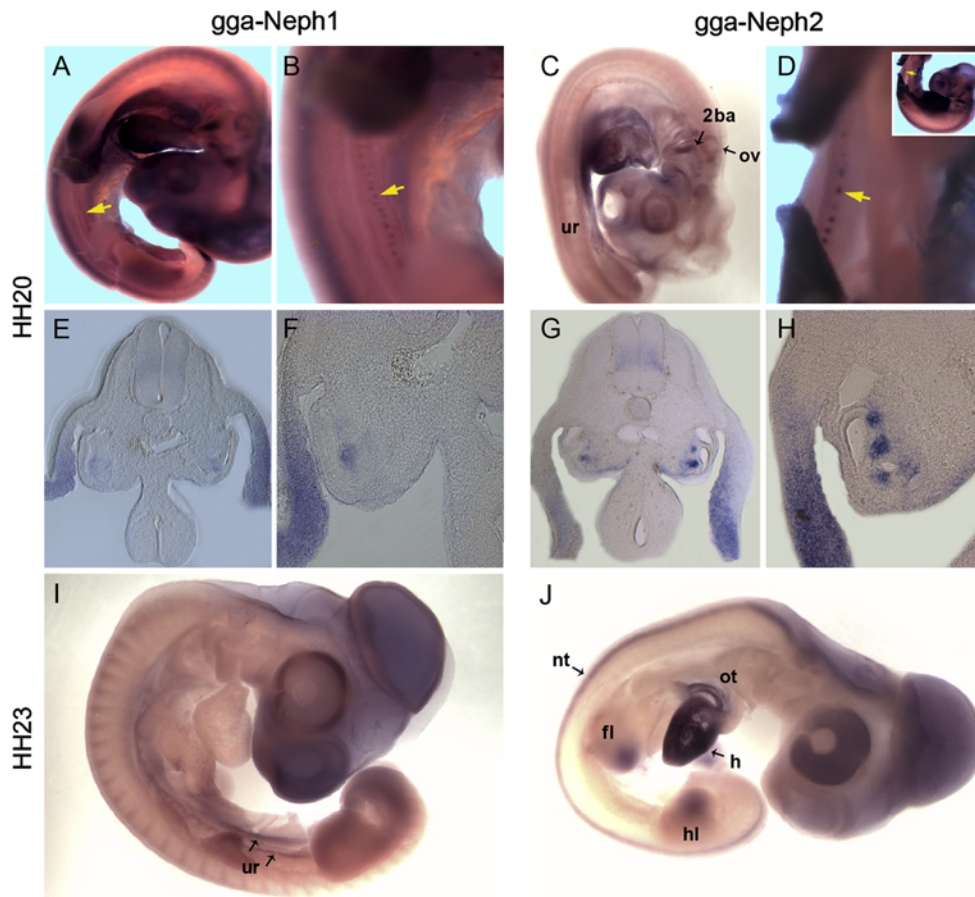


Fig. 6 Expression of *Neph1*- and *Neph2*-homologues during chicken embryo development. At stage HH20, *Neph1* and *Neph2* transcripts are detectable in the the mesonephros (yellow arrows in **a**, **b**, and **d**/Insert for orientation) and urogenital ride (**c**). Additional expression domains are found in the otic vesicle (**a**, **c**, **i**), the branchial arches (**a**, **c**), and the limb mesenchyme (**a**, **i**, **j**). On vibratome sections, the expression of *Neph1* and *Neph2* in the peri-Wolffian ductal mesonephric mesoderm

and in the lateral plate mesoderm is evident (**e**, **f**, **g**, **h**). At HH23, *Neph1* is expressed in the urogenital ridge and the limbs (**i**), whereas *Neph2* exhibits a broader expression pattern in the limbs, the heart and its outflow tract (**j**), and the neural tube (**g**, **j**). *2ba* second branchial arch, *fl* fore limb, *h* heart, *hl* hind limb, *nt* neural tube, *ov* otic vesicle, *ot* outflow tract, *ur* urogenital ridge

the mesonephric kidney starts at HH19 as a faint diffuse expression domain in the peri-Wolffian duct region (data not shown). From stage HH20 onwards, the staining intensity increased, and the tissue condensed into the maturing early pre-nephron vesicles and tubules appearing as beads-like structures along the mesonephric ridge. An additional expression domain was found in the lateral plate mesoderm. *Gga-Neph2* expression pattern at HH20 were seen in the developing nephrons adjacent to the Wolffian duct. This expression domain was broader and more prominent in the nephrogenic mesoderm in comparison to *gga-Neph1*. *Gga-Neph2* was expressed in the urogenital ridge at earlier stages (HH20) but expression was attenuated at later stages (HH23). Conversely, CNS expression had broadened by HH23 and extended into the neural crest, the mesencephalon, and the optic cup while none of these areas stained positive at HH20. In the second branchial arch, a dash-like cell cluster stains for *gga-Neph2* (Fig. 6c). Hind and fore limb

buds showed *gga-Neph* transcription in the apical and central parts of the bud but not at the base, while very strong expression in the developing heart remained consistent over time.

Discussion

In the present study, we showed that *Neph1-3* mRNAs are expressed in a wide range of vertebrate organ systems. Although some previous studies addressed *Neph* protein expression in development (Gerke et al. 2006; Hornberg et al. 2009; Komori et al. 2008; Morikawa et al. 2007; Serizawa et al. 2006), the present study for the first time provides a comprehensive analysis of *Neph* gene expression in mouse and chick development. Our study identified *Neph2* and *Neph3* mRNA expression in sensory organs like the olfactory epithelium and the otic vesicle consistent with previ-

ously reported results (Serizawa et al. 2006). Recent evidence suggested that Neph3-positive nerve terminals in the cochlea project onto Neph2-positive inner and outer hair cells, thus presenting a process that possibly requires Neph proteins for precise axonal projections onto target cells (Morikawa et al. 2007). Based on these observation and on data from *C. elegans* and *D. melanogaster* our results suggest that cell populations in the neocortex and the neuroepithelium, which give rise to the future neurohypophysis, might express Neph proteins as guidance cues for projecting axons. Neph2 and Neph3 are mutually exclusively expressed in neurons of the olfactory bulb together with axonal repellent Ephrin A5 and its tyrosine receptor kinase EphA5 (Serizawa et al. 2006). Moreover, the *Neph3* expression pattern in the spinal cord resembles that of EphA5 and EphrinA5 as previously reported (Fig. 1h, i) (Cooper et al. 2009; Yue et al. 1999). Here, EphA5 and EphrinA5 help to establish dorso-ventral patterning, and Neph3 could constitute a potential new player in this morphogenetic event. The ligand/receptor pair EphrinA5 and EphA5 also exerts influence on basal insulin secretion by pancreatic islet cells to regulate glucose homeostasis (Konstantinova et al. 2007). Since *Neph3* and *Neph2* have been shown to be expressed in the brain under the control of pancreatic transcription factor 1a (Ptf1a), and transcripts of both mRNAs have been detected in the pancreas, it is intriguing to surmise that Neph3 represents one part of another receptor/ligand pair that participates in fine-tuning insulin release (Nishida et al. 2010). This is further supported by the recent finding that Neph3 localizes to the plasma membrane of insulin vesicles of pancreatic beta cells (Fornoni et al. 2010).

Cell migration is another essential mechanism in ontogenesis and very similar to axonal pathfinding as it requires cell-bound or soluble factors for directional outgrowth and site-specific settling (Dickson 2002). Data from the fruit fly have already suggested a role for Neph proteins in cell migration and fusion (Ruiz-Gómez et al. 2000; Strunkelberg et al. 2001). In fact, many organs that depend on cells of high migratory activity during development stain positive for either *Neph1/2* or *Neph3* (i.e. neural crest, heart, neocortex, neurohypophysis, branchial arches). A strong *Neph2* signal was found in avian embryos beginning at stage HH20 in the heart and its outflow tract, which to some part derives from migrating neural crest cells. Therefore, it is conceivable that Neph proteins either contribute to directing neural crest cells to the heart anlage or help sorting cells to form the intricate structure of the outflow tract. In addition, branchial arches show *Neph1* and *Neph2* expression. From these structures, migrating neural crest cells later form a great variety of tissues ranging from bone to neurons and thymus. In the neurohypophysis, the migrating diencephalic neuroepithelium invaginates to form the infundibular stalk.

Neuron migration in the neocortex is essential to organize neurons in layers. Abrogation of the mechanism—e.g. in the reeler mouse mutant—leads to the disorganization of the layer structure (Frotscher et al. 2009; Goffinet 1979). A similar phenotype was observed when simultaneously knocking out the kinases *src* and *fyn* which are known to phosphorylate Neph3-Neph1 complexes to induce intracellular signaling (Kuo et al. 2005; Manto 2008). In combination with the expression patterns we observe in this study, this strongly suggests a role for Neph proteins in neo- and allocortical neuron migration. However, no severe neuronal phenotype has been observed in *Neph3* or *Neph1* knock-out animals (Donoviel et al. 2001; Putaala et al. 2001). The murine *Neph3* gene is specifically expressed in kidney, brain, and pancreas. Inactivation of the gene leads to massive proteinuria and neonatal death. In humans, however, *Neph3*-deficient patients display cerebellar ataxia in about 10% of all cases (Putaala et al. 2001), and a recent publication links *Neph2* to cases of intellectual disability (Bhalla et al. 2008).

Further, mutations in *CASK*, a downstream effector of Neph1 and Neph2, cause a brain malformation phenotype with microcephaly and hypoplasia of the brainstem and cerebellum (Gerke et al. 2006; Najm et al. 2008; Piluso et al. 2009; Tarpey et al. 2009). A possible explanation for the lack of an apparent neuronal phenotype in *Neph* mutants could be that immunoglobulin-superfamily molecules act in a redundant manner (Neumann-Haefelin et al. 2010). As a perspective, it would be of great interest to create double- or triple-knock-out animals for either *Neph1/2/3*, possibly in combination with *Neph3*, to screen for CNS defects.

Other functions of IgSF-proteins inferred from experiments in *Drosophila* include cell sorting and cell fate determination in morphogenesis. In the cerebellum, Ptf1a expression triggers *Neph3* expression and determines neuronal precursor cell fate by causing differentiation into GABAergic subpopulations (Hoshino et al. 2005; Mizuhara et al. 2010; Pascual et al. 2007). Similar processes might take place in some of the organs we report here to be positive for *Neph* mRNA expression. *Neph1* in the lung potentially promotes cell sorting during embryonic induction of epithelial ducts or contributes to the continuing interaction between the endodermal epithelium and the lung mesenchyme during organogenesis. We detected *Neph1* and *Neph2* transcripts in overlapping areas of the limb buds at synchronous time points (E11.5). Expression seems to specifically take place in the apical ectodermal ridge, which serves as a signaling center controlling limb mesenchyme proliferation and keeps mesenchymal cells in an undifferentiated state (Duboc and Logan 2009). Important effectors of limb development are fibroblast growth factors (FGFs), Hox-transcription factors, sonic hedgehog (Shh), and Wnt-signaling (Newman and Bhat

2007). They cooperate to establish dorso-ventral polarity, promote proliferation and growth, and trigger mesenchymal condensations, which in turn differentiate into muscles, bones, tendons, and cartilage. Concomitant *Neph* expression, thus, suggests a role in forming mesenchymal condensations similar to myoblast aggregation and fusion in *Drosophila*. It is also conceivable that by controlling cell affinity, they regulate the position and sorting of newly spawned cell populations during the outgrowth of the limb bud as proximal limb structures appear first and pertaining cells need to cluster accordingly. A comparable function has already been described for a structurally related protein N-cadherin giving positional identity to future cartilaginous elements of the limb (Tuan 2003; Yajima et al. 2002). Beyond that, Neph might provide survival signals to certain cell populations and prevent apoptosis, which is known to be an important morphogenetic factor. In our eyes, it would be worthwhile to see whether some of the well-characterized transcription factors involved in limb development differentially control *Neph* expression in the apical ectodermal ridge as well as other expression domains, as *Neph* genes seem to be controlled by different sets of transcription factors (Guo et al. 2004; Nishida et al. 2010; Ristola et al. 2009).

In addition to the data on rodent development, we present an expression analysis in chicken embryos. Homologues of *Neph* proteins have been described in a number of species ranging from fruit fly to nematodes, zebra fish, rodents, and humans (Fig. 5). So far, expression in *Gallus gallus* has not been reported. With the presented work, we add another species to the list of potential model organism in research on *Neph* gene function. In contrast to the mouse, the avian embryo is much better accessible in vivo and can be subjected to many well-described methods in developmental biology such as in vivo electroporation, microinjection, or in vivo time-lapse microscopy (Funahashi and Nakamura 2008; Wilson 1996). These options would greatly expand the methods available to basic molecular research on adhesion molecules of the *Neph* family. Our analyses show that the expression patterns in *Gallus gallus* closely mimic those in the mouse and suggest a common theme in *Neph* function.

In conclusion, our data suggest that *Neph*-dependent cell recognition may play a role in a variety of different tissues and organs in vertebrates. Future studies will help to address the role of these proteins in tissue morphogenesis by creating tissue- and organ-specific knock-out animals.

Acknowledgments We thank Stefanie Keller, Christina Engel, Charlotte Meyer and Petra Dämisch for excellent technical assistance, and members of the laboratories for helpful discussions. T.B. received funding through the Deutsche Forschungsgemeinschaft (BE2212, SFB572 and SFB635), B.S. received funding through the Deutsche Forschungsgemeinschaft (SCHE1562, SFB 832).

Open Access This article is distributed under the terms of the Creative Commons Attribution Noncommercial License which permits any noncommercial use, distribution, and reproduction in any medium, provided the original author(s) and source are credited.

References

- Bao S, Cagan R (2005) Preferential adhesion mediated by hibris and roughest regulates morphogenesis and patterning in the drosophila eye. *Dev Cell* 8:925–935. doi:10.1016/j.devcel.2005.03.011
- Barletta G-M, Kovari IA, Verma RK, Kerjaschki D, Holzman LB (2003) Nephrin and neph1 co-localize at the podocyte foot process intercellular junction and form cis hetero-oligomers. *J Biol Chem* 278:19266–19271. doi:10.1074/jbc.M301279200
- Bhalla K, Luo Y, Buchan T, Beachem MA, Guzauskas GF, Ladd S et al (2008) Alterations in CDH15 and KIRREL3 in patients with mild to severe intellectual disability. *Am J Hum Genet* 83:703–713. doi:S0002-9297(08)00555-7[pii]10.1016/j.ajhg.2008.10.020
- Chen EH, Olson EN (2004) Towards a molecular pathway for myoblast fusion in *Drosophila*. *Trends Cell Biol* 14:452–460. doi:10.1016/j.tcb.2004.07.008
- Clandinin TR, Zipursky SL (2002) Making connections in the fly visual system. *Neuron* 35:827–841 (pii:S0896627302008760)
- Cooper MA, Crockett DP, Nowakowski RS, Gale NW, Zhou R (2009) Distribution of EphA5 receptor protein in the developing and adult mouse nervous system. *J Comp Neurol* 514:310–328. doi:10.1002/cne.22030
- Dickson BJ (2002) Molecular mechanisms of axon guidance. *Science* 298:1959–1964. doi:10.1126/science.1072165
- Donoviel DB, Freed DD, Vogel H, Potter DG, Hawkins E, Barrish JP et al (2001) Proteinuria and perinatal lethality in mice lacking NEPH1, a novel protein with homology to NEPHRIN. *Mol Cell Biol* 21:4829–4836. doi:10.1128/MCB.21.14.4829-4836.2001
- Duboc V, Logan MP (2009) Building limb morphology through integration of signalling modules. *Curr Opin Genet Dev* 19:497–503. doi:10.1016/j.gde.2009.07.002
- Fischbach K-F, Linneweber GA, Andlauer TF, Hertenstein A, Bonengel B, Chaudhary K (2009) The irre cell recognition module (IRM) proteins. *J Neurogenet* 23:48–67. doi:10.1080/01677060802471668
- Fornoni A, Jeon J, Varona Santos J, Cobianchi L, Jauregui A, Inverardi L et al (2010) Nephrin is expressed on the surface of insulin vesicles and facilitates glucose-stimulated insulin release. *Diabetes* 59:190–199. doi:10.2337/db09-0655
- Frotscher M, Chai X, Bock HH, Haas CA, Förster E, Zhao S (2009) Role of Reelin in the development and maintenance of cortical lamination. *J Neural Transm* 116:1451–1455. doi:10.1007/s00702-009-0228-7
- Funahashi J, Nakamura H (2008) Electroporation in avian embryos. *Methods Mol Biol* 461:377–382. doi:10.1007/978-1-60327-483-8_27
- Gerke P, Huber TB, Sellin L, Benzing T, Walz G (2003) Homodimerization and heterodimerization of the glomerular podocyte proteins nephrin and NEPH1. *J Am Soc Nephrol* 14:918–926
- Gerke P, Sellin L, Kretz O, Petraschka D, Zentgraf H, Benzing T et al (2005) NEPH2 is located at the glomerular slit diaphragm, interacts with nephrin and is cleaved from podocytes by metalloproteinases. *J Am Soc Nephrol* 16:1693–1702. doi:10.1681/ASN.2004060439
- Gerke P, Benzing T, Hohne M, Kispert A, Frotscher M, Walz G et al (2006) Neuronal expression and interaction with the synaptic protein CASK suggest a role for Neph1 and Neph2 in synaptogenesis. *J Comp Neurol* 498:466–475. doi:10.1002/cne.21064

- Goffinet AM (1979) An early development defect in the cerebral cortex of the reeler mouse. *Anat Embryol* 157:205–216. doi:10.1007/BF00305160
- Guo G, Morrison DJ, Licht JD, Quaggin SE (2004) WT1 activates a glomerular-specific enhancer identified from the human nephrin gene. *J Am Soc Nephrol* 15:2851–2856. doi:10.1097/01.ASN.0000143474.91362.C4
- Hornberg M, Gussing F, Berghard A, Bohm S (2009) Retinoic acid selectively inhibits death of basal vomeronasal neurons during late stage of neural circuit formation. *J Neurochem* 110:1263–1275. doi:10.1111/j.1471-4159.2009.06216.x
- Hoshino M, Nakamura S, Mori K, Kawauchi T, Terao M, Nishimura YV et al (2005) Ptf1a, a bHLH transcriptional gene, defines GABAergic neuronal fates in cerebellum. *Neuron* 47:201–213. doi:10.1016/j.neuron.2005.06.007
- Hoveyda N, Shield JP, Garrett C, Chong WK, Beardsall K, Bentsi-Enchill E et al (1999) Neonatal diabetes mellitus and cerebellar hypoplasia/agenesis: report of a new recessive syndrome. *J Med Genet* 36:700–704
- Huber TB, Benzinger T (2005) The slit diaphragm: a signaling platform to regulate podocyte function. *Curr Opin Nephrol Hypertens* 14:211–216 (pii:00041552-200505000-00004)
- Ihalmo P, Palmén T, Ahola H, Valtonen E, Holthöfer H (2003) Filtrix is a novel member of nephrin-like proteins. *Biochem Biophys Res Commun* 300:364–370. doi:10.1016/S0006-291X(02)02854-1
- Kestila M, Lenkkeri U, Mannikko M, Lamerdin J, McCready P, Putaala H et al (1998) Positionally cloned gene for a novel glomerular protein—nephrin—is mutated in congenital nephrotic syndrome. *Mol Cell* 1:575–582 (pii:S1097-2765(00)80057-X)
- Komori T, Gyobu H, Ueno H, Kitamura T, Senba E, Morikawa Y (2008) Expression of kin of irregular chiasm-like 3/mKirre in proprioceptive neurons of the dorsal root ganglia and its interaction with nephrin in muscle spindles. *J Comp Neurol* 511:92–108. doi:10.1002/cne.21838
- Konstantinova I, Nikolova G, Ohara-Imaizumi M, Meda P, Kucera T, Zarbalis K et al (2007) EphA-ephrin-A-mediated beta cell communication regulates insulin secretion from pancreatic islets. *Cell* 129:359–370. doi:10.1016/j.cell.2007.02.044
- Kuo G, Arnaud L, Kronstad-O'Brien P, Cooper JA (2005) Absence of Fyn and Src causes a reeler-like phenotype. *J Neurosci* 25:8578–8586. doi:10.1523/JNEUROSCI.1656-05.2005
- Liu G, Kaw B, Kurfis J, Rahmanuddin S, Kanwar YS, Chugh SS (2003) Nephl and nephrin interaction in the slit diaphragm is an important determinant of glomerular permeability. *J Clin Invest* 112:209–221. doi:10.1172/jci.18242
- Maness PF, Schachner M (2007) Neural recognition molecules of the immunoglobulin superfamily: signaling transducers of axon guidance and neuronal migration. *Nat Neurosci* 10:19–26. doi:10.1038/nn1827
- Manto M (2008) The cerebellum, cerebellar disorders, and cerebellar research—two centuries of discoveries. *Cerebellum* 7:505–516. doi:10.1007/s12311-008-0063-7
- Menon SD, Osman Z, Chenchill K, Chia W (2005) A positive feedback loop between Dumbfounded and Rolling pebbles leads to myotube enlargement in *Drosophila*. *J Cell Biol* 169:909–920. doi:10.1083/jcb.200501126
- Minaki Y, Mizuhara E, Morimoto K, Nakatani T, Sakamoto Y, Inoue Y et al (2005) Migrating postmitotic neural precursor cells in the ventricular zone extend apical processes and form adherens junctions near the ventricle in the developing spinal cord. *Neurosci Res* 52:250–262
- Mizuhara E, Minaki Y, Nakatani T, Kumai M, Inoue T, Muguruma K et al (2010) Purkinje cells originate from cerebellar ventricular zone progenitors positive for Neph3 and E-cadherin. *Dev Biol* 338:202–214. doi:10.1016/j.ydbio.2009.11.032
- Morikawa Y, Komori T, Hisaoka T, Ueno H, Kitamura T, Senba E (2007) Expression of mKirre in the developing sensory pathways: its close apposition to nephrin-expressing cells. *Neuroscience* 150:880–886. doi:10.1016/j.neuroscience.2007.10.013
- Najm J, Horn D, Wimplinger I, Golden JA, Chizhikov VV, Sudi J et al (2008) Mutations of CASK cause an X-linked brain malformation phenotype with microcephaly and hypoplasia of the brainstem and cerebellum. *Nat Genet*. doi:10.1038/ng.194
- Neumann-Haefelin E, Kramer-Zucker A, Slanchev K, Hartleben B, Noutsou F, Martin K et al (2010) A model organism approach: defining the role of Neph proteins as regulators of neuron and kidney morphogenesis. *Hum Mol Genet* 19:2347–2359. doi:10.1093/hmg/ddq108
- Newman SA, Bhat R (2007) Activator-inhibitor dynamics of vertebrate limb pattern formation. *Birth Defects Res C Embryo Today* 81:305–319. doi:10.1002/bdrc.20112
- Nishida K, Hoshino M, Kawaguchi Y, Murakami F (2010) Ptf1a directly controls expression of immunoglobulin superfamily molecules Nephrin and Neph3 in the developing central nervous system. *J Biol Chem* 285:373–380. doi:10.1074/jbc.M109.060657
- Pascual M, Abasolo I, Mingorance-Le Meur A, Martínez A, Del Rio JA, Wright CVE et al (2007) Cerebellar GABAergic progenitors adopt an external granule cell-like phenotype in the absence of Ptf1a transcription factor expression. *Proc Natl Acad Sci USA* 104:5193–5198. doi:10.1073/pnas.0605699104
- Piluso G, D'Amico F, Saccone V, Bismuto E, Rotundo IL, Di Domenico M et al (2009) A missense mutation in CASK causes FG syndrome in an Italian family. *Am J Hum Genet* 84:162–177. doi:10.1016/j.ajhg.2008.12.018
- Putaala H, Soininen R, Kilpelainen P, Wartiovaara J, Tryggvason K (2001) The murine nephrin gene is specifically expressed in kidney, brain and pancreas: inactivation of the gene leads to massive proteinuria and neonatal death. *Hum Mol Genet* 10:1–8
- Ramos RG, Igloi GL, Lichte B, Baumann U, Maier D, Schneider T et al (1993) The irregular chiasm C-roughest locus of *Drosophila*, which affects axonal projections and programmed cell death, encodes a novel immunoglobulin-like protein. *Genes Dev* 7:2533–2547
- Ristola M, Arpiainen S, Saleem MA, Mathieson PW, Welsh GI, Lehtonen S et al (2009) Regulation of Neph3 gene in podocytes—key roles of transcription factors NF-kappaB and Sp1. *BMC Mol Biol* 10:83. doi:10.1186/1471-2199-10-83
- Ruiz-Gómez M, Coutts N, Price A, Taylor MV, Bate M (2000) *Drosophila* dumbfounded: a myoblast attractant essential for fusion. *Cell* 102:189–198
- Schneider T (1995) Restricted expression of the irrc-rst protein is required for normal axonal projections of columnar visual neurons. *Neuron* 15:259–271. doi:10.1016/0896-6273(95)90032-2
- Sellick GS, Barker KT, Stolte-Dijkstra I, Fleischmann C, Coleman RJ, Garrett C et al (2004) Mutations in PTF1A cause pancreatic and cerebellar agenesis. *Nat Genet* 36:1301–1305. doi:10.1038/ng1475
- Sellin L, Huber TB, Gerke P, Quack I, Pavenstädt H, Walz G (2003) NEPH1 defines a novel family of podocin interacting proteins. *FASEB J* 17:115–117. doi:10.1096/fj.02-0242fj
- Serizawa S, Miyamichi K, Takeuchi H, Yamagishi Y, Suzuki M, Sakano H (2006) A neuronal identity code for the odorant receptor-specific and activity-dependent axon sorting. *Cell* 127:1057–1069. doi:10.1016/j.cell.2006.10.031
- Shen K, Fetter RD, Bargmann CI (2004) Synaptic specificity is generated by the synaptic guidepost protein SYG-2 and its receptor, SYG-1. *Cell* 116:869–881 (pii:S0092867400251X)
- Strunkelberg M, Bonengel B, Moda LM, Hertenstein A, de Couet HG, Ramos RG et al (2001) rst and its paralogue kirre act redundantly

- during embryonic muscle development in *Drosophila*. *Development* 128:4229–4239
- Sugie A, Umetsu D, Yasugi T, Fischbach KF, Tabata T (2010) Recognition of pre- and postsynaptic neurons via nephrin/NEPH1 homologs is a basis for the formation of the *Drosophila* retinotopic map. *Development* 137:3303–3313
- Tarpey PS, Smith R, Pleasance E, Whibley A, Edkins S, Hardy C et al (2009) A systematic, large-scale resequencing screen of X-chromosome coding exons in mental retardation. *Nat Genet* 41:535–543. doi:[10.1038/ng.367](https://doi.org/10.1038/ng.367)
- Tuan RS (2003) Cellular signaling in developmental chondrogenesis: N-cadherin, Wnts, and BMP-2. *J Bone Joint Surg Am* 85(A Suppl 2):137–141
- Wilson LM (1996) *Methods in Cell Biology*. Academic Press, London
- Yajima H, Hara K, Ide H, Tamura K (2002) Cell adhesiveness and affinity for limb pattern formation. *Int J Dev Biol* 46:897–904
- Young HM, Anderson RB, Newgreen DF (2009) Neural Crest. In: Lemke G (ed) *Developmental Neurobiology*, 1st edn. Academic Press, London, pp 271–281
- Yue Y, Su J, Cerretti DP, Fox GM, Jing S, Zhou R (1999) Selective inhibition of spinal cord neurite outgrowth and cell survival by the Eph family ligand ephrin-A5. *J Neurosci* 19:10026–10035